agronomy

MDPI

Article

Synergistic Effects of Biodegradable Nano-Plastics and Salt Stress on Maize Seedling Growth and Physiology

Yuyang Li [1], Huiying Li [1], Chunfeng Xie [2], Zhuangzhuang Hong [3], Jing Liu [1], Shuaijie Jin [1], Yan Chen [1], Yunlu Wang [1], Zhanqiang Ma [1], Aneela Younas [1], Muhammad Shaaban [1], Yanfang Wang [1,*] and Ling Liu [1,*]

[1] College of Agriculture, Henan University of Science and Technology, Luoyang 471000, China; yuyangl@stu.haust.edu.cn (Y.L.)
[2] Zhangjiajie Municipal Bureau of Agriculture and Rural Affairs, Zhangjiajie 427000, China
[3] National Kay Laboratory of Crop Genetic Improvement, Huazhong Agricultural University, Wuhan 430070, China
* Correspondence: 9903024@haust.edu.cn (Y.W.); liuling1978@haust.edu.cn (L.L.)

Abstract

The accumulation of polylactic acid nano-plastics (PLA-NPs) in saline–alkali soils poses a potential threat to crop growth; however, the underlying toxicological mechanisms remain poorly understood. We conducted a hydroponic experiment to investigate the effects of polylactic acid (PLA) NPs (100 and 500 mg L^{-1}) under conditions both in the presence (50 mmol L^{-1} NaCl) and absence of salt stress on maize seed germination, seedling growth, physiological characteristics, and transcriptomic responses. The results showed that exposure to PLA-NPs, particularly at a high concentration (500 mg L^{-1}), significantly inhibited seed germination and seedling growth. Compared to the low concentration (100 mg L^{-1}) of PLA-NPs, the high concentrations (500 mg L^{-1}) reduced the germination percentage by 25.0% and fresh weight by 25.8% and increased root MDA (6.7%), SOD (30.0%), POD (6.3%), ASA (13.4%), and GSH (13.1%). Under the same concentration of the PLA, PLA + NaCl treatments exerted stronger inhibitory effects than PLA-NPs alone, with the seed germination percentage and fresh weight reduced by an average of 52.7% and 6.6%, respectively. Notably, the inhibitory effects and integrated biomarker response (IBR) index of the PLA 500 + NaCl treatment were the highest. The presence of PLA-NPs in roots was confirmed using confocal laser scanning microscopy. GO enrichment analysis showed that pathways related to nutrient reservoir activity, oxidoreductase activity, hydrogen peroxide catabolic process, and hydrogen peroxide metabolic process were enriched under PLA-NP and PLA + NaCl treatments. KEGG analysis further indicated enrichment in phenylpropanoid biosynthesis, ABC transporters, and alpha-linolenic acid metabolism. The PLA-NP and PLA + NaCl treatments upregulated genes associated with oxidoreductase activity (Zm00001eb238800, Zm00001eb128620, and Zm00001eb020790). These findings suggest that synergistic toxicity of PLA-NPs and salinity stress in maize is primarily driven by the internalization of PLA-NPs and Na^+ within maize roots, which negatively impacts maize seed germination and seedling growth by disrupting redox homeostasis and metabolic balance, thereby forcing plants to reallocate resources from growth toward oxidative stress defense. This study provides critical insights into the environmental risks of biodegradable nano-plastics in saline–alkali soil environments.

Keywords: polylactic acid nano-plastics; salt stress; maize; synergistic toxicity; oxidative stress; transcriptomic response

Check for updates

Academic Editor: Marco Betti

Received: 19 May 2026
Revised: 16 June 2026
Accepted: 18 June 2026
Published: 21 June 2026

Copyright: © 2026 by the authors. Licensee MDPI, Basel, Switzerland. This article is an open access article distributed under the terms and conditions of the Creative Commons Attribution (CC BY) license.

1. Introduction

Plastic particles are typically classified into micro-plastics (MPs, diameter < 5 mm) and nano-plastics (NPs, diameter ranging from 1 nm to 1 μm) [1]. As a newly recognized environmental pollutant, NPs have garnered significant attention. In recent years, biodegradable polymers such as polylactic acid (PLA) have been widely applied in agricultural systems as alternatives to traditional agricultural mulches [2]. Compared with conventional micro-plastics, biodegradable MPs are more readily utilized by soil microorganisms and play a positive role in various chemical processes, thereby influencing the cycling and sequestration of soil carbon (C) [3]. However, some studies indicate that polylactic acid (PLA) plastics persist in soil for extended periods due to their slow degradation rates, which can adversely affect soil ecology and crop development [4–6]. Due to their unique physicochemical properties, NPs have greater mobility and accumulation potential than MPs, facilitating their interactions with other environmental pollutants [7]. Chen et al. [8] reported that NPs could adsorb onto soil pollutants and may alter soil microbial community structure and function, affecting soil fertility and diversity. Additionally, NPs can be absorbed by plant roots and transported to aboveground tissues via the transpiration stream [9], leading to greater phytotoxicity than MPs by traversing cell membranes and inducing cellular damage [10–12].

Soil salinization is a significant challenge for global agriculture productivity and soil health, particularly in China [13]. Salinized soil has poor physical structure and aeration, is compacted, and exhibits reduced water retention, which hinders improvements in soil fertility and crop yields [14]. Furthermore, salt stress induces osmotic imbalance in plant cells, ion toxicity (notably Na^+ accumulation), and metabolic disorders [15]. Excessive Na^+ disrupts the intracellular Na^+/K^+ equilibrium, hindering the uptake of essential nutrients and accelerating the accumulation of reactive oxygen species (ROS), which ultimately interferes with enzymatic activities and physiological functions [16–18]. Ju et al. [19] reported that plastic film mulching is widely used in saline–alkali soils to mitigate salinity stress and conserve soil moisture. However, studies have shown that long-term mulched drip irrigation has not only led to salt accumulation in the plow layer, affecting soil structure and nutrient cycling [20], but also increased the accumulation of MPs in soil [19]. Plastic film mulching represents a major source of micro-plastic pollution in agricultural soils [8]. The ecological impact of micro-plastics in saline–alkali soils is influenced by various factors, including their type, concentration, size, and interaction with salt [21]. The combined stress of MPs and NaCl has been reported to increase ROS levels and reduce photosynthetic capacity in maize seedlings [22]. Xu et al. [21] suggested that MPs may not exhibit synergistic toxicity with salt regarding plant growth. Significant progress has been made in understanding the impact of plastic pollution on soil ecosystems, but research on the synergistic effects of MP pollution and salt stress on crops remains in its infancy. It is therefore necessary to investigate the mechanisms underlying the combined effects of PLA-NPs and salinity on maize, in order to provide a theoretical basis for enhancing crop productivity in saline-alkali soils.

Maize is the most important food crop in China and plays a crucial role in ensuring food security [23]. The individual effects of polylactic acid nanoparticles (PLA-NPs) and salt stress on maize have been extensively studied, but the mechanisms underlying their co-exposure remain unclear. Therefore, we selected maize as a model crop to investigate the response mechanisms to PLA-NPs under both in the presence and absence of salt stress. We employed a combined approach of physiological trait analysis, confocal laser scanning microscopy (CLSM), and transcriptome sequencing to investigate the following questions: (1) whether PLA nanoparticles and NaCl exert a synergistic inhibitory effect on seed germination and seedling growth; (2) whether salinity stress promotes PLA-NPs

accumulation in root tissues; and (3) how maize regulates antioxidant and defense-related pathways at the molecular level in response to combined stress. This study aims to provide mechanistic insights for evaluating the migration, accumulation patterns, and ecological risks of biodegradable plastics in saline-affected agricultural ecosystems.

2. Materials and Methods

2.1. Plant and Nano-Plastic Materials

Maize (*Zea mays* L. cv. Yuke 256) was used for this experiment. We purchased the monodisperse fluorescently labeled polylactic acid (PLA) nanospheres (50 nm in diameter, 545/572 nm) from Jiangsu Zhichuan Technology Co., Ltd. (Nantong, China).

2.2. Experimental Treatments

Seeds of uniform size were sterilized in 10% H_2O_2 for 20 min, rinsed thoroughly with distilled water, and soaked in distilled water for 24 h. Fifteen seeds per replicate were positioned in a 9 cm Petri dish lined with filter paper and treated with 10 mL of treatment solutions (Figure 1a). Five treatments were applied, with four replicates for each treatment: (1) no PLA-NPs and NaCl (CK); (2) PLA-NP concentration of 100 mg L^{-1} (PLA100); (3) PLA-NP concentration of 500 mg L^{-1} (PLA500); (4) PLA-NP concentration of 100 mg L^{-1} and NaCl concentration of 50 mmol L^{-1} (PLA100 + NaCl); (5) PLA-NP concentration of 500 mg L^{-1} and NaCl concentration of 50 mmol L^{-1} (PLA500 + NaCl). To ensure the uniform dispersion of the PLA nanospheres (PLA-NPs) in distilled water and prevent aggregation, the nanosphere suspension was subjected to ultrasonic treatment for 20 min at 25 °C using an SB25-12DT ultrasonicator (Ningbo Scientz Biotechnology Co., Ltd., Ningbo, China). The control treatment consisted of no PLA-NPs or NaCl. Cultures were maintained at 28 °C in darkness. Distilled water was added daily based on weight loss to compensate for evaporation losses and maintain a constant solution concentration.

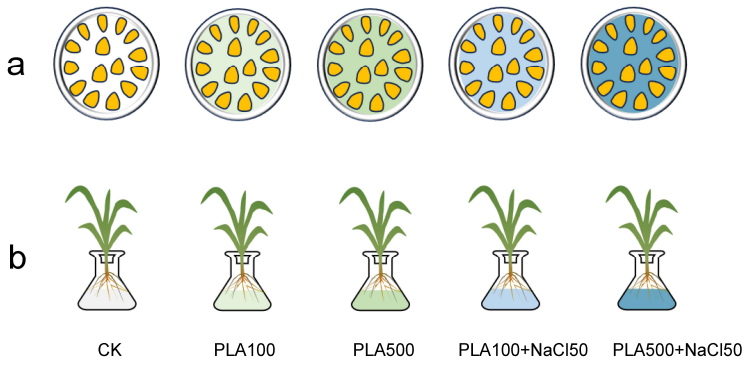


Figure 1. Hydroponic maize diagram. (**a**) Treatments of maize seed germination; (**b**) Treatments of maize seedling growth.

After 10 days of seed germination, uniform seedlings were anchored with cotton and transferred into 100 mL conical flasks, which contained 50 mL of modified Hoagland's nutrient solution (Figure 1b). There were five treatments, CK, PLA 100, PLA 500, PLA 100 + NaCl, and PLA 500 + NaCl, with six replicates for each treatment. To simulate the dark soil environment, flasks were wrapped in aluminum foil. Each treatment consisted of 12 biological replicates (two seedlings per flask). Throughout the exposure period, the nutrient solution was replaced every 3 days to maintain a stable concentration. The maize seedlings were grown in controlled environmental conditions (a 14/10 h light/dark photoperiod and day/night temperature of 28/20 °C). This experiment was conducted at Henan University of Science and Technology from 3 to 21 November 2024.

2.3. Seed Germination Parameters

Seed germination was monitored daily. The germinated seeds (defined as seeds in which the radicle protruded through the seed coat by at least 2 mm) were recorded until the number of germinated seeds in the Petri dish remained unchanged. The following formulae were used to calculate the seed germination parameters:

$$\text{Germination percentage (GP)} = \frac{\text{Number of seeds germinated in the first 7 days}}{\text{Total number of test seeds}} \times 100\% \quad (1)$$

$$\text{Germination index (GI)} = \sum \frac{\text{Gt}}{\text{Dt}} \quad (2)$$

$$\text{Vigor index (VI)} = \text{GI} \times \text{S} \quad (3)$$

In these equations, Gt denotes the number of germinated seeds on day t, Dt denotes the corresponding germination time (days), and S indicates the average seedling length measured at the end of the germination test.

2.4. The Observation of Confocal Laser Scanning Microscope

After 7 days of exposure to PLA nanospheres, root samples were collected, washed with distilled water, and given ultrasonic treatment for 10 min to remove any PLA particles. Fresh maize roots were manually cut using a blade to prepare transverse maize root sections [9]. The fluorescently labeled polylactic acid (PLA) nanospheres within maize root tissues were observed by using a confocal laser scanning microscope (FluoView FV3000, Olympus, Tokyo, Japan) at excitation/emission wavelengths of 545/572 nm.

2.5. Sample Collection and Analysis

2.5.1. Measurement of Maize Fresh Weight

Maize tissues were collected for fresh weight determination and measured using six plants per treatment. An electronic balance was used to measure the fresh weight. Maize leaves and roots were frozen in liquid nitrogen then stored at −80 °C until use.

2.5.2. Measurement of MDA Content

The malondialdehyde (MDA) content in maize was measured by the thiobarbituric acid method [24] and expressed in μmol g^{-1} FW.

2.5.3. Measurement of Antioxidant Enzyme Activities

The NBT method [25] was used to measure superoxide dismutase (SOD) activity. SOD activity was calculated using 50% inhibition of NBT photoreduction as one unit of enzyme activity and was expressed in U g^{-1} FW. The guaiacol method [9] was used to measure peroxidase (POD) activity. POD activity was calculated using a 0.01 change in A_{470} per minute as one unit of peroxidase activity (U) and was expressed in U g^{-1} min^{-1} FW. Catalase (CAT) activity was measured by the reduction of H_2O_2 at 240 nm within 3 min [9] and expressed in U g^{-1} min^{-1} FW.

2.5.4. Measurement of Antioxidant Content

The antioxidant contents of ASA and GSH were measured according to the method of Karam et al. [26] and Hussain et al. [27], respectively, and expressed in μmol g^{-1} FW.

2.6. Integrated Biomarker Response

The integrated biomarker response (IBR) index was calculated to integrate the multivariate biomarker data into a single value representing the overall stress level. The analysis was performed in R (version 4.5.2) using the IBRtools package. First, the raw data for each

biomarker were standardized (Z-score normalization) using the mean and standard deviation of the control group as the reference. Subsequently, the IBR index for each treatment group was computed, which geometrically represents the area of a star plot. The results are presented as the mean IBR index ± standard deviation for each treatment, and the star plot patterns were visually compared to assess differential biomarker responses.

2.7. RNA Sequencing of Expressed Genes in Maize Roots

Root samples were sequenced at Shanghai Majorbio Bio-pharm Biotechnology Co., Ltd. (Shanghai, China). On the Illumina NovaSeq X Plus platform, cDNA libraries were constructed and sequenced. The quality of the filtered data was validated with a Q30 percentage ranging from 89.38% to 90.03%. The high-quality reads were then aligned to the maize reference genome (Zm-B73-REFERENCE-NAM-5.0) using HISat2 (Version 2.1.0).

The Majorbio Cloud Platform was used for differential expression analysis. RSEM was employed to calculate the read counts for gene expression quantification [28]. Differentially expressed genes (DEGs) were identified using DESeq2, with screening criteria of log 2-fold change ≥ 1 and $p < 0.05$ [29]. Functional enrichment analyses, including Gene Ontology (GO) and Kyoto Encyclopedia of Genes and Genomes (KEGG), were conducted using GOatools (https://github.com/tanghaibao/GOatools (accessed on 15 June 2026)) and Python scipy software (https://scipy.org/install/ (accessed on 15 June 2026)), respectively. GO terms were considered significantly enriched at a false discovery rate (FDR) < 0.05, while KEGG pathways were considered significantly enriched at $p < 0.05$.

2.8. Statistical Analysis

All experimental data were processed using Microsoft Excel 2019 and analyzed with Duncan's test for the ANOVA using SPSS 25.0 to verify the significant difference among all treatments ($p < 0.05$). Origin 2026 was used for correlation analysis, and Adobe Illustrate 2024 was used for drawing.

3. Results

3.1. Synergistic Effects of PLA-NPs and Salt Stress on Maize Seed Germination and Seedling Growth

The effects of PLA-NPs alone (PLA) and in combination with NaCl (PLA + NaCl) on maize seed vigor were investigated (Figure 2). Exposure to PLA-NPs, either alone or in combination with NaCl, inhibited maize seed germination. Compared to the control (CK), the inhibitory effect of 500 mg·L^{-1} PLA-NPs (PLA500) was significantly more pronounced than that of 100 mg·L^{-1} PLA-NPs (PLA100). The co-exposure of PLA and NaCl further enhanced this inhibition, indicating a potentially synergistic toxic effect. Compared with PLA100, PLA100 + NaCl decreased the germination percentage, germination index, and vigor index by 48.4–70.1%. Compared to PLA500, PLA500 + NaCl decreased these indices by 35.0–57.0%. Overall, these results indicate that salt stress significantly enhanced the toxic effects of PLA-NPs on the germination of maize seeds.

The effect of PLA-NPs alone (PLA) and in combination with NaCl (PLA + NaCl) on maize seedling growth was also investigated. Both PLA and PLA + NaCl treatments inhibited the fresh weight of maize seedlings. Compared with CK, the growth inhibition effect of 500 mg·L^{-1} PLA-NPs (PLA500) was significantly higher than that of 100 mg·L^{-1} PLA-NPs (PLA100). For PLA100 and PLA500, the fresh weight decreased by 27.8% and 46.4%, respectively. The PLA + NaCl treatments further intensified the inhibition of seedling growth. Compared with PLA100, PLA100 + NaCl significantly decreased fresh weight by 17.5%. The combination of PLA500 + NaCl had no significant effect on fresh weight.

These results showed that salt stress enhanced the phytotoxicity of PLA toward maize seedling growth.

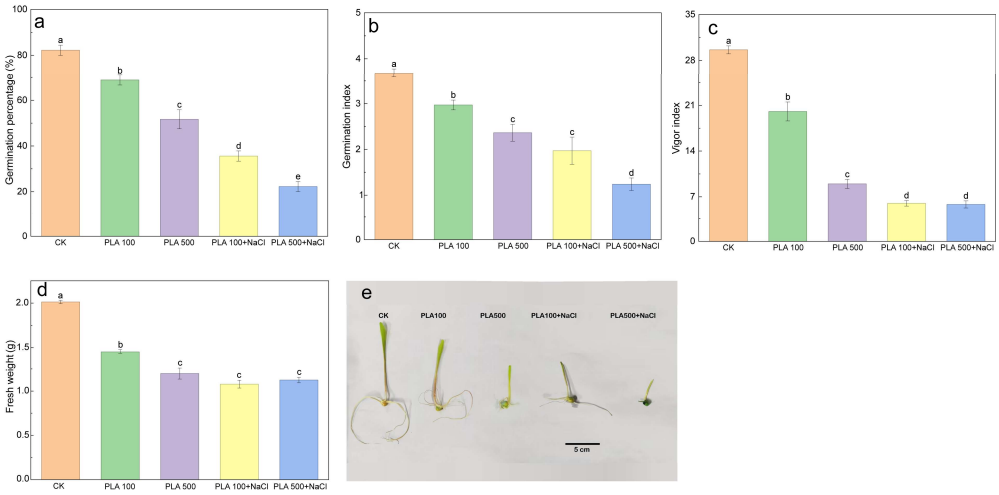


Figure 2. Synergistic effects of PLA-NPs and salt stress on maize seed germination.:(**a**–**e**) demonstrate germination percentage, germination index, vigor index, fresh weight and figure of seed germination. CK, PLA100, PLA500, PLA100 + NaCl, and PLA500 + NaCl demonstrate no PLA-NPs and NaCl; PLA-NP concentration of 100 mg L^{-1}; PLA-NP concentration of 500 mg L^{-1}; PLA-NP concentration of 100 mg L^{-1} and NaCl concentration of 50 mmol L^{-1}; PLA-NP concentration of 500 mg L^{-1} and NaCl concentration of 50 mmol L^{-1}, respectively. Values are means of replicates ± standard error. The bars with different lowercase letters indicate significant differences among the treatments ($p < 0.05$).

3.2. Absorption and Distribution of PLA Nano-Plastics in Maize Roots

In the fluorescence labeling experiment using nano-plastics, maize roots were capable of absorbing PLA-NPs (Figure 3). The CK treatment had no fluorescence signal in the roots of maize. We observed significant fluorescence signals within the intercellular spaces and cell wall gaps. There were differences in absorption and distribution. The PLA + NaCl treatments exhibited stronger signals and tended to form aggregated clusters within intercellular spaces compared to PLA-alone treatments. Under salt stress, PLA500 exhibited more fluorescent signals in the root stele compared to PLA100. These results showed that the maize root could absorb PLA-NPs and that salt stress might enhance this uptake and promote their aggregation in the root.

3.3. Synergistic Effects of PLA-NPs and Salt Stress on Antioxidant Enzyme Activity of Maize

The effects of PLA-NPs alone (PLA) and in combination with NaCl (PLA + NaCl) on the antioxidant system of maize seedlings were studied (Figure 4). Both PLA and PLA + NaCl treatments significantly increased MDA content, antioxidant enzyme activities, and antioxidant content. Compared with CK, the MDA content of PLA500 was higher than that of PLA100. Exposure to PLA100 and PLA500 increased the MDA content in roots by 22.3% and 30.5%, respectively. The MDA contents of PLA + NaCl were higher than PLA-NPs alone. Compared with PLA100, PLA100 + NaCl increased the MDA content in roots and leaves by 36.1% and 6.1%. Compared with PLA500, PLA500 + NaCl increased the MDA content in roots and leaves by 45.7% and 27.4%.

The antioxidant enzyme activities and antioxidant content were significantly increased. For instance, compared with CK, exposure to PLA100 and PLA500 increased the activities of SOD, POD, and CAT in roots by 28.3%, 13.9%, and 47.6% and 66.7%, 21.1%, and 119.1%, respectively. Compared with PLA alone, the combined treatments significantly increased the stimulation of CAT activity in leaves and GSH content in roots. These results show

that co-exposure to PLA-NPs and salt stress promotes ROS accumulation, suppresses ASA content, and increases oxidative stress in maize seedlings.

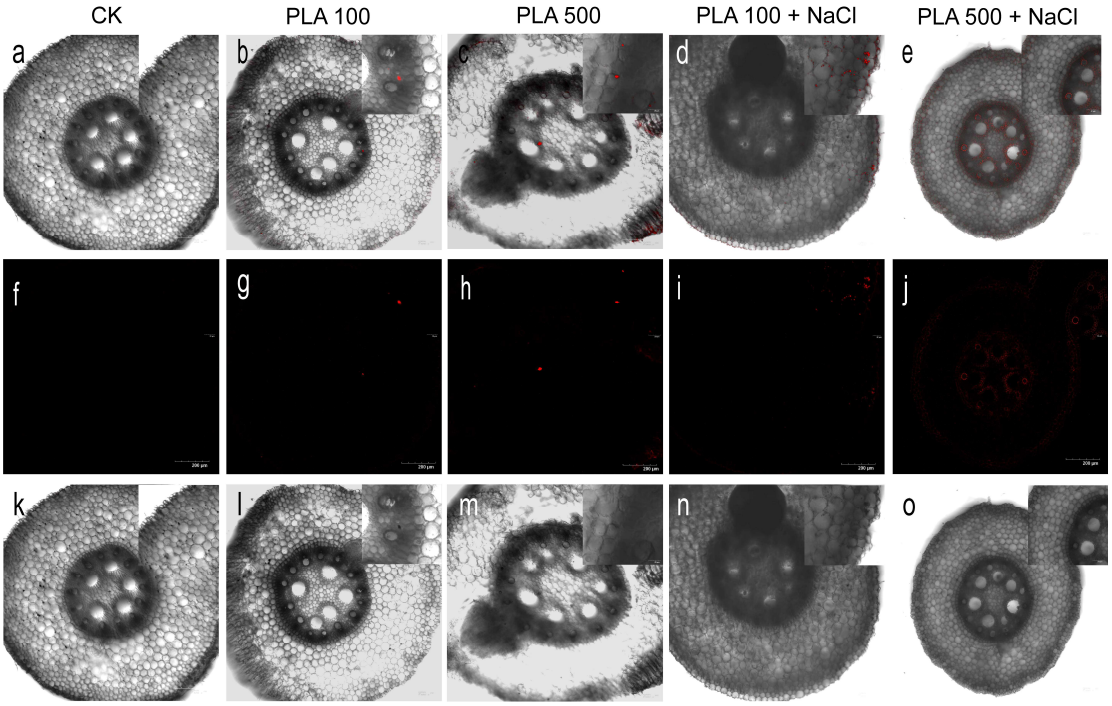


Figure 3. Confocal microscopic images of the maize root surface after 7 days of exposure to different treatments: (**a**–**e**) are the corresponding merged images of bright-field images and fluorescent images; (**f**–**j**) are fluorescent images; and (**k**–**o**) are bright-field images. CK, PLA100, PLA500, PLA100 + NaCl, and PLA500 + NaCl demonstrate no PLA-NPs and NaCl; PLA-NP concentration of 100 mg L^{-1}; PLA-NP concentration of 500 mg L^{-1}; PLA-NP concentration of 100 mg L^{-1} and NaCl concentration of 50 mmol L^{-1}; PLA-NP concentration of 500 mg L^{-1} and NaCl concentration of 50 mmol L^{-1}, respectively.

3.4. Integrated Biomarker Responses (IBR)

Six biomarkers (SOD, POD, CAT, MDA, ASA, and GSH) were analyzed using the IBR approach, and IBR star plots were constructed (Figure 5a,b). The radar chart area under the PLA 500 + NaCl treatment was the largest, indicating the strongest oxidative stress response. The oxidative stress response in leaves across different treatments followed the order PLA 500 + NaCl > PLA 500 > PLA 100 + NaCl > PLA 100 > CK. In the PLA100 treatment, SOD, ASA, and GSH dominated in maize leaves but POD, CAT, and ASA dominated in maize roots. In the PLA500 treatment, SOD, POD, and ASA dominated in maize leaves but SOD, POD, and CAT dominated in maize roots. In the PLA100 + NaCl treatment, SOD, POD, CAT, and GSH dominated in maize leaves but SOD, MDA, ASA, and GSH dominated in maize roots. In the PLA500 + NaCl treatment, MDA, ASA, and GSH dominated in maize leaves but SOD, MDA, ASA, and GSH dominated in maize roots. The IBR index of PLA and salt stress was analyzed (Figure 5c,d). Compared with CK, the IBR index of PLA-NPs alone (PLA) and in combination with NaCl (PLA + NaCl) was high, and that of the PLA500 + NaCl treatment was the highest. The IBR indices of different treatments were PLA500 + NaCl > PLA500 > PLA100 + NaCl > PLA100 > CK.

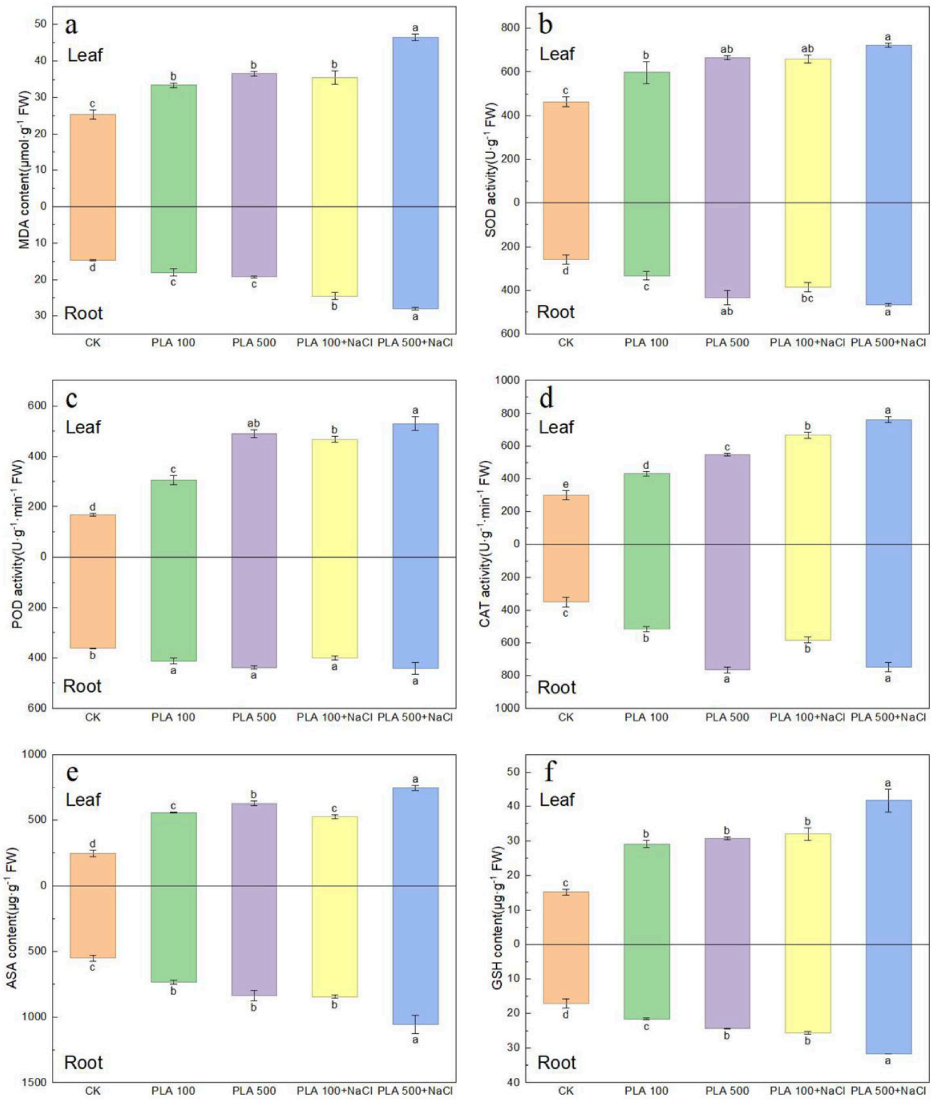


Figure 4. Synergistic effects of PLA-NPs and salt stress on enzymes activity of maize: (**a**–**f**) demonstrate MDA content, SOD activity, POD activity, CAT activity, ASA content and GSH content, respectively. CK, PLA100, PLA500, PLA100 + NaCl, and PLA500 + NaCl demonstrate no PLA-NPs and NaCl; PLA-NP concentration of 100 mg L^{-1}; PLA-NP concentration of 500 mg L^{-1}; PLA-NP concentration of 100 mg L^{-1} and NaCl concentration of 50 mmol L^{-1}; PLA-NP concentration of 500 mg L^{-1} and NaCl concentration of 50 mmol L^{-1}, respectively. Values are means of replicates ± standard error. The bars with different lowercase letters indicate significant differences among the treatments ($p < 0.05$).

3.5. Transcriptome Analysis of PLA-NPs and Salt Stress on Maize Roots

The differentially expressed genes (DEGs) in maize under different treatments are shown (Figure 6). The total number of DEGs across CK, PLA100, PLA500, PLA100 + NaCl, and PLA500 + NaCl was 18,372, and the number of DEGs was 341, 246, 123, 261, and 382, respectively (Figure 6a). The number of shared DEGs across all treatments was 61 (Figure 6b). Compared with CK, the number of unique DEGs in PLA100, PLA500, PLA100 + NaCl, and PLA500 + NaCl was 106, 289, 217, and 2243, respectively. The results showed that PLA-NPs significantly alter gene expression profiles in maize roots under both the presence and absence of salt stress.

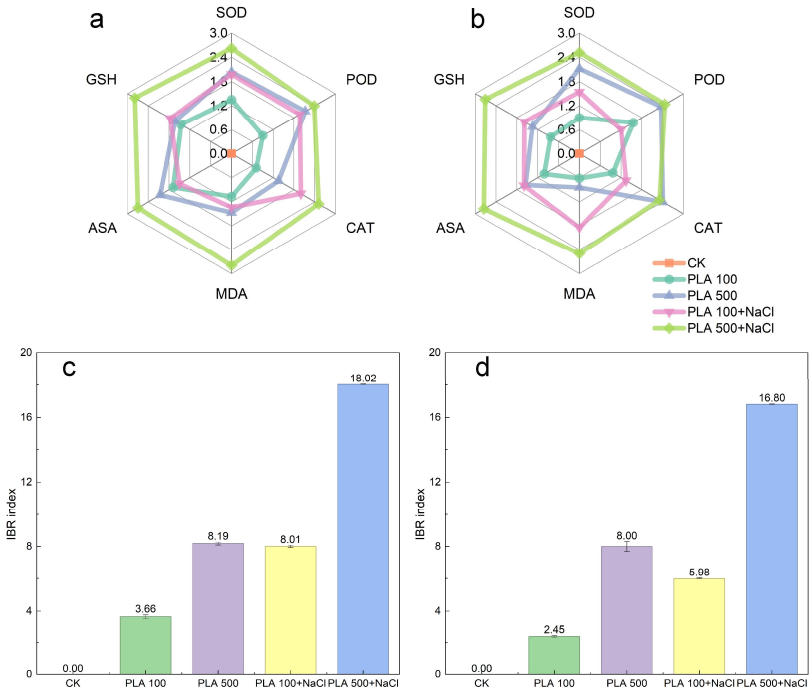


Figure 5. IBR star plot (**a**,**b**) and IBR index (**c**,**d**) of maize seedlings responding to PLA-NPs and salt stress: (**a**,**c**) indicate the IBR radar chart and the IBR index of the leaf, and (**b**,**d**) indicate the IBR radar chart and the IBR index of the root. CK, PLA100, PLA500, PLA100 + NaCl, and PLA500 + NaCl demonstrate no PLA-NPs and NaCl; PLA-NP concentration of 100 mg L^{-1}; PLA-NP concentration of 500 mg L^{-1}; PLA-NP concentration of 100 mg L^{-1} and NaCl concentration of 50 mmol L^{-1}; PLA-NP concentration of 500 mg L^{-1} and NaCl concentration of 50 mmol L^{-1}, respectively. The radar chart area represents the comprehensive level of oxidative stress: a larger area indicates a stronger oxidative stress response induced by PLA and salt stress.

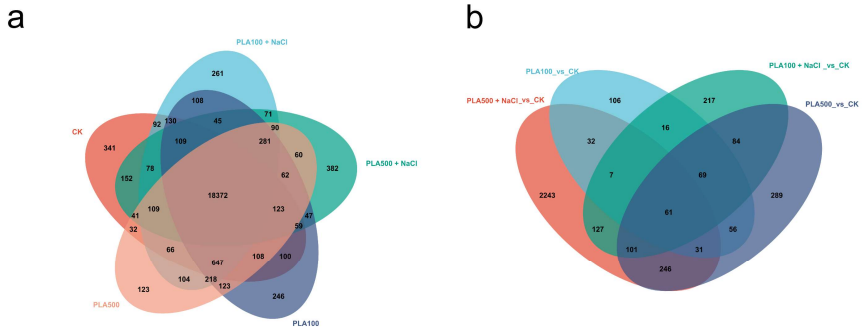


Figure 6. Venn map analysis of DEGs in maize. (**a**) The DEGs of different treatments. (**b**) Compared with CK, the number of share and unique DEGs in PLA100, PLA500, PLA100 + NaCl, and PLA500 + NaCl. CK, PLA100, PLA500, PLA100 + NaCl, and PLA500 + NaCl demonstrate no PLA-NPs and NaCl; PLA-NP concentration of 100 mg L^{-1}; PLA-NP concentration of 500 mg L^{-1}; PLA-NP concentration of 100 mg L^{-1} and NaCl concentration of 50 mmol L^{-1}; PLA-NP concentration of 500 mg L^{-1} and NaCl concentration of 50 mmol L^{-1}, respectively.

We used volcano plots to study the distribution of DEGs (Figure 7). More significant differences and a higher level of variation were observed in PLA500 compared with CK than in PLA100. Compared with CK, PLA100 upregulated 138 genes and downregulated 606 genes, while PLA500 upregulated 454 genes and downregulated 1318 genes. Compared with CK, PLA100 + NaCl upregulated 307 genes and downregulated 1073 genes, while PLA500 + NaCl upregulated 1091 genes and downregulated 2201 genes. More significant differences and a higher level of variation were observed in co-exposure treatments compared with CK than in PLA alone treatments. In the PLA100 + NaCl vs. PLA100

comparison, 27 genes were upregulated and 34 genes were downregulated. However, in the PLA500 + NaCl vs. PLA500 comparison, 884 and 923 genes were upregulated and downregulated, respectively.

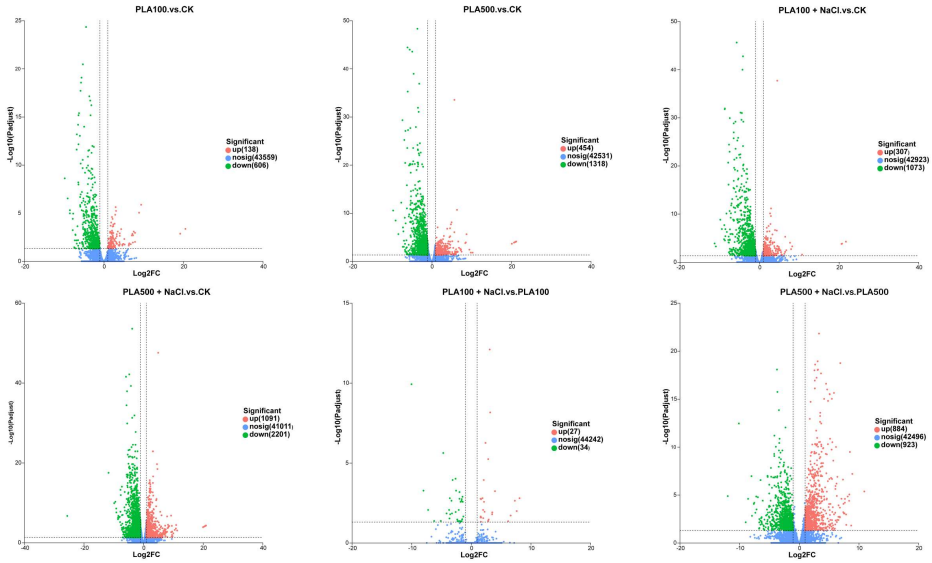


Figure 7. Volcano map analysis of differentially expressed genes under different treatments. CK, PLA100, PLA500, PLA100 + NaCl, and PLA500 + NaCl demonstrate no PLA-NPs and NaCl; PLA-NP concentration of 100 mg L^{-1}; PLA-NP concentration of 500 mg L^{-1}; PLA-NP concentration of 100 mg L^{-1} and NaCl concentration of 50 mmol L^{-1}; PLA-NP concentration of 500 mg L^{-1} and NaCl concentration of 50 mmol L^{-1}, respectively.

3.6. GO and KEGG Enrichment Analysis of DEGs

All DEGs were analyzed using Gene Ontology (GO) (Figure 8a) analysis. GO enrichment analysis revealed some common enriched pathways activated in all treatments, including for the extracellular region (GO:0005576), cell wall (GO:0005618), apoplast (GO:0048046), external encapsulating structure (GO:0030312), nutrient reservoir activity (GO:0045735), oxidoreductase activity (GO:0016491), lactoperoxidase activity (GO:0140825), hydrogen peroxide catabolic process (GO:0042744), and hydrogen peroxide metabolic process (GO:0042743).

Transcriptome analysis further indicated that PLA treatments enriched GO terms related to cellular detoxification and peroxidase activity. More GO items of detoxification (GO:0098754), abscisic acid transport (GO:0080168), and mitochondrial cytochrome c oxidase assembly (GO:0033617) were enriched in PLA100 roots. Compared with PLA100, the PLA500 treatment showed a broader enrichment profile. PLA500 uniquely affected the plasma membrane (GO:0005886), response to oxidative stress (GO:0006979), and heme binding (GO:0020037). PLA500 displayed increased enrichment of oxidoreductase-related molecular functions, including oxidoreductase activity, acting on peroxide as an acceptor (GO:0016684) and peroxidase activity (GO:0004601). The combined PLA100 + NaCl treatment further enhanced the oxidative defense system, including antioxidant activity (GO:0016209), defense response (GO:0006952), and cellular oxidant detoxification (GO:0098869). Under the PLA500 + NaCl treatment, the enrichment was more complex. More GO items of protein phosphorylation (GO:0006468), DNA-binding transcription factor activity (MF, GO:0003700), and cell wall organization (GO:0071555) were enriched in PLA500 + NaCl. These results indicate that high-concentration combined stress exerts a significant impact on cellular signaling pathways and structural components.

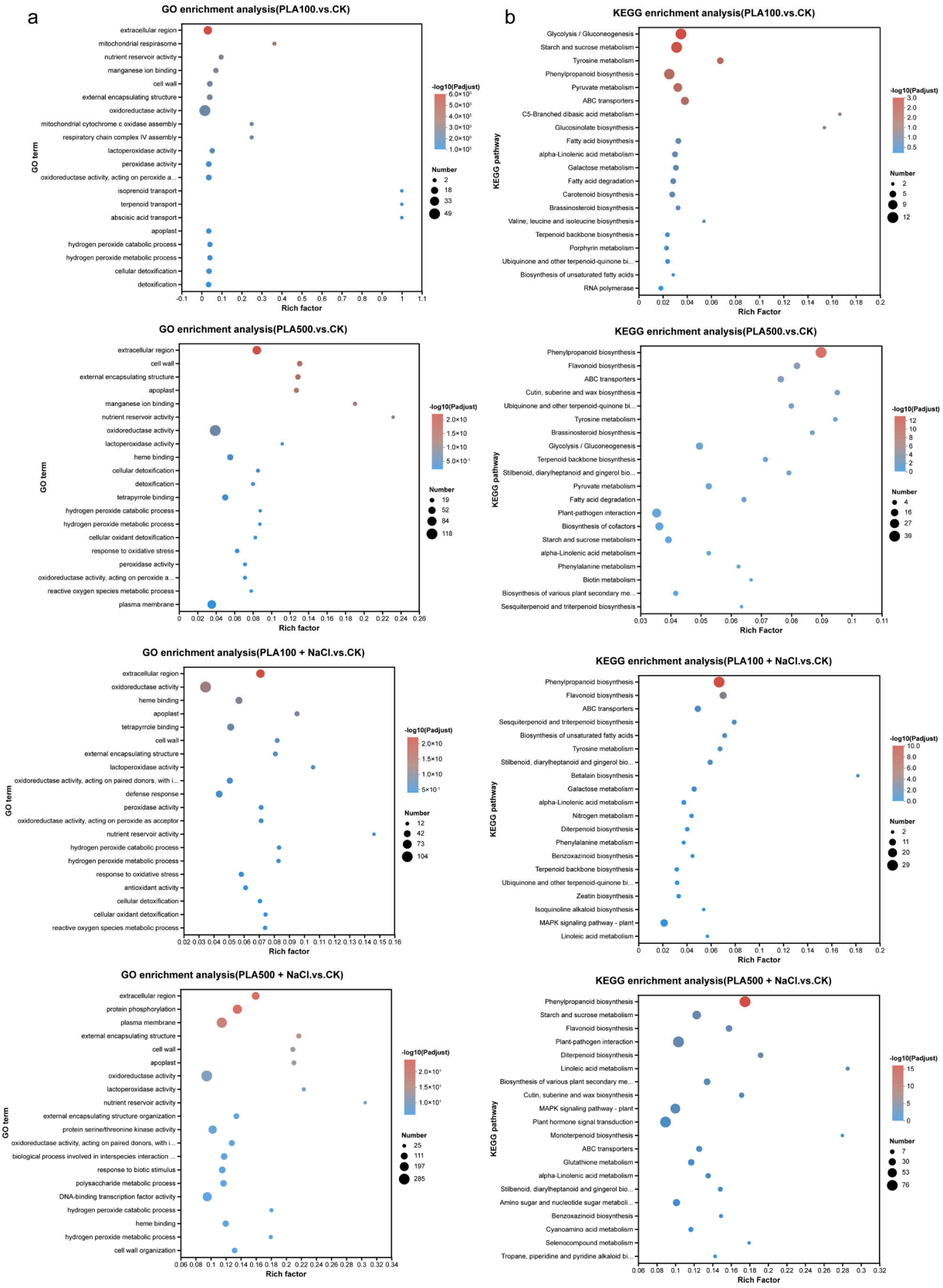


Figure 8. GO (**a**) and KEGG (**b**) enrichment analyses of differentially expressed genes under different treatments. CK, PLA100, PLA500, PLA100 + NaCl, and PLA500 + NaCl demonstrate no PLA-NPs and NaCl; PLA-NP concentration of 100 mg L^{-1}; PLA-NP concentration of 500 mg L^{-1}; PLA-NP concentration of 100 mg L^{-1} and NaCl concentration of 50 mmol L^{-1}; PLA-NP concentration of 500 mg L^{-1} and NaCl concentration of 50 mmol L^{-1}, respectively.

Figure 8b shows Kyoto Encyclopedia of Genes and Genomes (KEGG) pathway analysis under different treatments. The KEGG data showed that DEGs of all treatments were mainly enriched in phenylpropanoid biosynthesis (zma00940), ABC transporters (zma02010), and alpha-linolenic acid metabolism (zma00592). The PLA100 treatment enriched pathways related to fatty acid biosynthesis (zma00061), carotenoid biosynthesis (zma00906), and valine, leucine and isoleucine biosynthesis (zma00290). Compared with CK, the pathways such as flavonoid biosynthesis (zma00941), sesquiterpenoid and triterpenoid biosynthesis (zma00909), and plant–pathogen interaction (zma04626) were enriched in PLA500. The MAPK signaling pathway—plant (zma04016) and nitrogen metabolism (zma00910) were enriched in PLA100 + NaCl. In contrast, MAPK signaling pathway—plant (zma04016), glutathione metabolism (zma00480), monoterpenoid biosynthesis (zma00902), and plant hormone signal transduction (zma04075) were enriched in PLA500 + NaCl.

Class III peroxidases (PRXs) are a class of peroxidase genes unique to plants that play a key role in maize growth, development, and stress responses. Analysis of genes involved in phenylpropanoid biosynthesis revealed that the expression of PRXs (Zm00001eb238800, Zm00001eb128620, and Zm00001eb020790) varied significantly among different treatments (Figure 9a). Both PLA-NPs and PLA + NaCl treatments increased PRX gene expression compared to CK, with the PLA500 + NaCl treatment showing the highest expression levels. Compared with CK, the expression level in PLA500 was higher than in PLA100. Compared to PLA-NPs alone, the combined PLA + NaCl treatments significantly upregulated PRX gene expression.

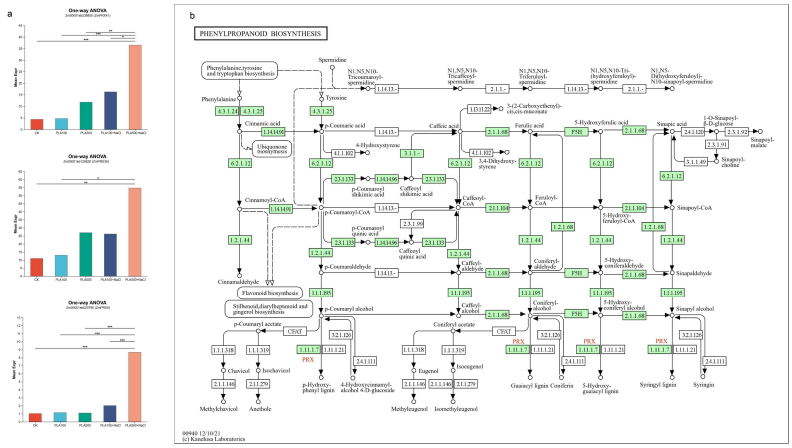


Figure 9. Effects of different treatments on the DEGs related to phenylpropanoid biosynthesis: (**a**,**b**) indicate expression differences of different treatments and phenylpropanoid biosynthesis, respectively. Solid lines represent direct interactions or direct enzymatic conversions; dashed lines indicate indirect interactions or multi-step processes. The green boxes indicate genes or enzymes that have been identified in the genome of maize and are linked to KEGG gene entries. CK, PLA100, PLA500, PLA100 + NaCl, and PLA500 + NaCl demonstrate no PLA-NPs and NaCl; PLA-NP concentration of 100 mg L^{-1}; PLA-NP concentration of 500 mg L^{-1}; PLA-NP concentration of 100 mg L^{-1} and NaCl concentration of 50 mmol L^{-1}; PLA-NP concentration of 500 mg L^{-1} and NaCl concentration of 50 mmol L^{-1}, respectively. "*", "**", and "***"denote $0.01 < p \leq 0.5$, $0.001 < p \leq 0.01$, $p \leq 0.001$.

4. Discussion

Micro-plastics (MPs) have been shown to delay seed germination, inhibit plant growth, and induce ecotoxicity and genotoxicity in plants [30–32]. In this study, we found that exposure to polylactic acid (PLA) nano-plastics (NPs) significantly inhibited seed germination. High concentrations of PLA-NPs had significantly greater inhibitory effects on the germination percentage, germination index, and vigor index than low concentrations. This

is consistent with previous reports [33,34]. The toxic effect likely stems from the accumulation of NPs within seed epidermal pores, which hinder water and nutrient uptake, thereby disrupting the germination process [30]. We observed strong fluorescent signals in maize roots via confocal microscopy, further demonstrating that PLA-NPs enter the root tissue, causing physical blockage and exerting direct toxic effects on cells. The toxicity of NPs may be amplified by their surface adsorption properties. We observed that combined treatment of polylactic acid (PLA) nano-plastics with NaCl stress exhibited a stronger inhibitory effect on seed vigor than PLA alone. This phenomenon may be attributed to NPs adsorbing salt ions, which disrupts ionic balance and thereby exacerbates physiological stress [35]. The vigor index of PLA 500 + NaCl was the lowest but did not differ significantly from PLA 100 + NaCl. This suggests that the stress of PLA 500 + NaCl may have approached the critical point for seed germination tolerance. When the stress on the seeds exceeded their self-regulation capacity, the activity of protective enzymes decreased significantly, causing the seeds to lose viability [33]. The PLA500 + NaCl treatment had the greatest inhibitory effect on seed germination, indicating that PLA500 exerts strong toxic stress under high concentrations, such as the highest MDA content, leading to the most severe inhibitory effects on germination. This effect may stem from high-concentration PLA accumulation within seed pores, more severe oxidative stress, or enhanced ion toxicity induced by its adsorption of salt ions [21,22,30,36].

Our results demonstrate that PLA and PLA + NaCl stress during the seed germination stage exerted a persistent inhibitory effect on maize seedling growth, significantly reducing germination percentages while also causing substantial declines in biomass. This indicates that physiological damage and metabolic disruption during early germination continuously interfered with nutrient uptake and resource allocation in seedlings, thereby limiting their vegetative growth [37]. The IBR index of roots under PLA500 + NaCl was 2.1-fold higher than that under PLA500, accompanied by higher MAD, ASA, and GSH levels. This suggests that PLA combined with salt stress more readily activates the hydrogen peroxide metabolic pathway, thereby enhancing oxidative stress responses. We further found that the co-enrichment of pathways related to nutrient reserve activity and hydrogen peroxide degradation across all treatment groups suggests a coordinated reallocation of carbon and energy reserves toward sustaining the antioxidant defense network. At the transcriptome level, maize appears to mobilize storage-derived metabolites (e.g., starch and sucrose metabolism genes) while regulating detoxification systems (SOD, POD, CAT, ASA, and GSH), thereby maintaining redox homeostasis under PLA- and NaCl-associated stresses. Therefore, we believe that plants face a trade-off between investment in molecular defense repertoires and growth [38,39], i.e., maize expends substantial stored energy and substances to maintain antioxidant defense system stability, thereby reducing resources available for growth. This energy allocation trade-off represents one of the key intrinsic mechanisms by which plants adapt to abiotic stress [40].

We used confocal laser scanning microscopy (CLSM) to reveal distinct fluorescent signals within the root tissues, confirming that PLA nano-plastics penetrate the root barrier. Bosker et al. [30] considered that this internal accumulation likely causes physical blockage of transport channels and directly exerts toxic effects on cellular structures [41,42]. Our study indicated that the fluorescence intensity was significantly amplified in the combined PLA + NaCl treatments compared to PLA alone. This may be because Na^+ could promote accumulation of PLA in the root, upsetting ion homeostasis and thereby exerting synergistic toxicity on plant growth, such as increasing MDA content and antioxidant enzyme activities. However, Xu et al. [21] reported no synergistic toxicity between micro-plastics and salinity in maize. Our results are different, likely due to differences in exposure systems (hydroponics vs. soil), particle size (50 nm in this study), or specific chemical properties of

the PLA polymer. Furthermore, unlike Wang et al. [7] and Zhang et al. [43], reporting the promoting effects of growth at low concentrations, all PLA treatments in this study (with a minimum concentration of 100 mg L^{-1}) showed inhibitory effects. This may be related to the smaller size (50 nm) and the higher starting concentration of PLA.

Excess ROS triggers membrane lipid peroxidation, resulting in the enhancement of the MDA content. Under PLA-alone treatments, MDA content in both leaves and roots significantly increased with increasing PLA concentration, and the PLA500 treatment exhibited the highest MDA content. Exposure to NPs commonly triggers oxidative stress, leading to excessive ROS accumulation and subsequent lipid peroxidation of cell membranes [44]. Combined treatments significantly elevated MDA content in both leaves and roots, with the highest content observed under the highest concentration treatment (PLA500 + NaCl). Salt stress further exacerbates this effect through osmotic and ionic stress, causing severe oxidative damage to organelles and, ultimately, leading to programmed cell and plant death [45]. To mitigate these detrimental effects of ROS, plants have evolved a series of antioxidants and antioxidant enzymes to scavenge reactive oxygen species and reduce cellular toxicity [46,47]. Co-exposure to PLA and NaCl significantly stimulated the antioxidant defense system in maize. Compared with the control (CK), PLA + NaCl treatments showed elevated activities of antioxidant enzymes (SOD, POD, and CAT) and increased non-enzymatic antioxidants (ASA and GSH). These findings indicate that co-exposure to PLA-NPs and NaCl stimulated greater oxidative stress, thereby activating antioxidant defense mechanisms in maize. Consistent with preliminary studies [9], NP exposure significantly increased both antioxidant enzyme activity and MDA content, and the toxic effect of NPs alone or combined with organic compounds leads to elevated ROS levels, which promote increased expression of antioxidant enzyme genes [48]. From the transcriptomic analysis it was found that the PLA-NP and PLA + NaCl treatments upregulated genes associated with oxidoreductase activity (Zm00001eb238800, Zm00001eb128620, and Zm00001eb020790). Liu et al. [22] also discovered that NaCl exacerbated the effects of NPs in maize and had significant toxic effects on seedling growth and the antioxidant system. SOD converts O_2 into hydrogen peroxide (H_2O_2), whose levels are regulated by the activities of POD and CAT [49]. Consistent with this, we found that the GO pathways of the hydrogen peroxide catabolic process and the hydrogen peroxide metabolic process were enriched, indicating that maize upregulates its antioxidant enzyme system at the genetic level to defend against oxidative damage.

Further transcriptomic analyses revealed that PLA-NPs affected gene expression across multiple biological functions and processes, and that different treatments (PLA alone or combined with NaCl) induced distinct transcriptional responses in maize. Our results showed that some GO terms and KEGG pathways were enriched in all treatments, pointing to a common response mechanism to PLA alone or combined with NaCl treatments. This was including the enrichment of the phenylpropanoid biosynthesis pathway, which promotes the production of phenolic compounds and lignin to mitigate oxidative stress, consistent with findings by Liu et al. [22]. Concomitantly, the enrichment of the GO term nutrient reservoir activity suggests that maize mobilizes stored reserves to sustain this defense-oriented biosynthesis, thereby diverting resources away from growth and providing a gene-expression-level explanation for the observed growth inhibition [38,50]. The enrichment of GO terms related to oxidoreductase activity, hydrogen peroxide catabolic process, and hydrogen peroxide metabolic process indicates that maize modulates hydrogen peroxide-centered reactive oxygen species metabolism by enhancing antioxidant enzyme activity [51], thereby alleviating the physiological stress induced by PLA and salt. The molecular response was highly specific to the stress intensity. Low-concentration PLA (PLA100) preferentially activated hormone signaling pathways (e.g., abscisic acid

transport and mitochondrial cytochrome c oxidase assembly) to adjust metabolic balance. High-concentration PLA (PLA500) triggered a systemic oxidative stress response (response to oxidative stress and reactive oxygen species metabolic process) and secondary metabolite biosynthesis. Moreover, PLA500 had more DEGs than PLA100, which may be the reason for the stronger toxicity of PLA500 on maize. Furthermore, the introduction of salt (NaCl) produced a clear synergistic effect with PLA. It is likely that the physical damage caused by PLA, combined with the ionic/osmotic stress induced by NaCl, likely led to greater cellular damage and/or a higher release of endogenous danger signals. Excessive ROS levels can overwhelm the antioxidant system, leading to lipid peroxidation and inhibiting plant growth. Consistent with this, the MDA content was significantly higher in the PLA500 treatment compared to the PLA100 treatment. Moreover, the high-concentration combination (PLA500 + NaCl) activated glutathione metabolism and plant–pathogen interaction pathways. This suggests that the severe physical and chemical damage caused by high-concentration NPs and salt is perceived by the plant similarly to a pathogen invasion, triggering complex immune responses like the MAPK cascade [49]. In conclusion, maize seedlings reallocate resources to phenylpropanoid biosynthesis and enhanced antioxidant defense systems, leading to inhibited seedling growth.

5. Conclusions

This study shows that polylactic acid nano-plastics (PLA-NPs), both in the presence and absence of salinity stress, were internalized into maize roots, significantly affecting seed germination, early seedling growth, physiological responses, and transcriptomic regulation in maize, with stronger effects observed on combined exposure. Higher PLA-NP concentrations (500 $mg \cdot L^{-1}$) caused greater growth inhibition than lower concentrations (100 $mg \cdot L^{-1}$), while co-exposure with NaCl further exacerbated these adverse effects. Co-exposure to salinity stress intensified oxidative damage and disrupted antioxidant system homeostasis compared with PLA-NPs alone. Transcriptomic analysis indicated that maize reprogrammed metabolic allocation toward stress-responsive pathways under both individual and combined treatments, particularly those related to phenylpropanoid biosynthesis, redox regulation, and signaling processes. Notably, the PLA + NaCl treatments further amplified oxidative damage and significantly enriched pathways related to oxidoreductase activity and MAPK signaling, highlighting the strong interaction between nano-plastic and salinity stress. Collectively, these findings demonstrate that PLA-NPs exacerbate salinity-induced stress through enhanced root uptake, disruption of ion homeostasis, and activation of ROS-related metabolic and signaling pathways. This study provides novel insights into the combined toxicity of nano-plastics and salinity stress in maize and offers a scientific basis for ecological risk assessment in agricultural systems.

Author Contributions: Conceptualization, Y.L.; methodology, H.L., J.L. and S.J.; software, Y.L.; validation, C.X. and L.L.; formal analysis, Y.L., Y.C. and Y.W. (Yunlu Wang); investigation, Y.C. and Z.H.; resources, Z.M., Y.W. (Yanfang Wang) and L.L.; writing—original draft, Y.L.; writing—review and editing, A.Y., M.S., Y.W. (Yanfang Wang) and L.L. All authors have read and agreed to the published version of the manuscript.

Funding: This work was supported by the National Natural Science Foundation of China (31700367) and the Scientific and Technological Research Projects in Henan Province (262102111097 and 242102110189).

Institutional Review Board Statement: Not applicable.

Data Availability Statement: The original contributions presented in this study are included in the article. Further inquiries can be directed to the corresponding authors.

Acknowledgments: During the preparation of this work, we used DeepL (https://www.deepl.com/translator) and Deepseek (https://chat.deepseek.com) for writing assistance (e.g., grammar, structure, spelling, punctuation, and formatting). After using these tools, the authors reviewed and edited the translated content to ensure its accuracy and coherence with the original findings. No AI tools were used for generating text, data, graphics, study design; data collection, analysis, or interpretation of data; or any other core scientific process. The authors take full responsibility for the final content of this publication.

Conflicts of Interest: The authors declare no conflicts of interest.

References

1. Hartmann, N.B.; Hüffer, T.; Thompson, R.C.; Hassellöv, M.; Verschoor, A.; Daugaard, A.E.; Rist, S.; Karlsson, T.; Brennholt, N.; Cole, M.; et al. Are We Speaking the Same Language? Recommendations for a Definition and Categorization Framework for Plastic Debris. *Environ. Sci. Technol.* **2019**, *53*, 1039–1047. [CrossRef] [PubMed]
2. Boots, B.; Russell, C.W.; Green, D.S. Effects of Microplastics in Soil Ecosystems: Above and Below Ground. *Environ. Sci. Technol.* **2019**, *53*, 11496–11506. [CrossRef] [PubMed]
3. Chen, L.Y.; Han, L.F.; Wang, F.Y.; Chen, Q.A.; Huang, H.K.; Wang, J.; Ma, C.X.; Sun, K.; Rillig, M.C.; Kuzyakov, Y.; et al. Polylactic acid microplastics induced negative priming and improved carbon sequestration via microbial processes in different paddy soils. *Soil Biol. Biochem.* **2025**, *201*, 109653. [CrossRef]
4. Xie, Z.W.; Men, C.; Yuan, X.; Miao, S.; Sun, Q.Y.; Hu, J.M.; Zhang, Y.Y.; Liu, Y.X.; Zuo, J.N. Naturally aged polylactic acid microplastics stunted pakchoi (*Brassica rapa* subsp. *chinensis*) growth with cadmium in soil. *J. Hazard. Mater.* **2023**, *460*, 132318. [CrossRef] [PubMed]
5. Yu, Y.X.; Lin, S.Y.; Sarkar, B.; Wang, J.; Liu, X.H.; Wang, D.N.; Ge, T.; Li, Y.Y.; Zhu, B.; Yao, H.Y. Mineralization and microbial utilization of poly(lactic acid) microplastic in soil. *J. Hazard. Mater.* **2024**, *476*, 135080. [CrossRef] [PubMed]
6. Zhao, Z.Y.; Wang, P.Y.; Wang, Y.B.; Zhou, R.; Koskei, K.; Munyasya, A.N.; Liu, S.T.; Wang, W.; Su, Y.Z.; Xiong, Y.C. Fate of plastic film residues in agro-ecosystem and its effects on aggregate-associated soil carbon and nitrogen stocks. *J. Hazard. Mater.* **2021**, *416*, 125954. [CrossRef] [PubMed]
7. Wang, C.C.; Luo, Q.; Zhang, J.L.; Zhang, X.Y.; Yang, N.; Feng, L.S. Toxic effects of microplastics and nanoplastics on plants: A global meta-analysis. *Environ. Pollut.* **2023**, *337*, 122593. [CrossRef] [PubMed]
8. Chen, L.; Qiu, T.; Huang, F.; Zeng, Y.; Cui, Y.; Chen, J.; White, J.C.; Fang, L. Micro/nanoplastics pollution poses a potential threat to soil health. *Glob. Change Biol.* **2024**, *30*, e17470. [CrossRef] [PubMed]
9. Li, Y.Y.; Huang, X.Y.; Lv, Q.; Ma, Z.Q.; Zhang, M.H.; Liu, J.; Fan, L.; Yan, X.J.; Jiao, N.Y.; Younas, A.; et al. Visual Observation of Polystyrene Microplastics/Nanoplastics in Peanut Seedlings and Their Effects on Growth and the Antioxidant Defense System. *Agronomy* **2025**, *15*, 1895. [CrossRef]
10. Li, L.Z.; Luo, Y.M.; Li, R.J.; Zhou, Q.; Peijnenburg, W.J.G.M.; Yin, N.; Yang, J.; Tu, C.; Zhang, Y.C. Effective uptake of submicrometre plastics by crop plants via a crack-entry mode. *Nat. Sustain.* **2020**, *3*, 929–937. [CrossRef]
11. Sun, X.D.; Yuan, X.Z.; Jia, Y.B.; Feng, L.J.; Zhu, F.P.; Dong, S.S.; Liu, J.J.; Kong, X.P.; Tian, H.Y.; Duan, J.L.; et al. Differentially charged nanoplastics demonstrate distinct accumulation in Arabidopsis thaliana. *Nat. Nanotechnol.* **2020**, *15*, 755–760. [CrossRef] [PubMed]
12. Zhu, W.Z.; Lu, S.Y.; Jiang, H.B.; Wang, P.; He, C.G.; Bian, H.F.; Wang, J.Y. Interactions between phenanthrene and polystyrene micro/nano plastics: Implications for rice (*Oryza sativa* L.) toxicity. *Environ. Pollut.* **2023**, *337*, 122360. [CrossRef] [PubMed]
13. Liu, X.D.; Wang, Z.S.; Shi, G.Y.; Gao, Y.B.; Zhang, H.; Liu, K.C. Effects of microplastics and salt single or combined stresses on growth and physiological responses of maize seedlings. *Physiol. Plant.* **2025**, *177*, e70106. [CrossRef] [PubMed]
14. Shi, X.L.; Guo, P.; Chen, Y.X.; Liu, C.; Liu, C.J.; Yu, H.Q.; Zhou, Y.F.; Zou, H.T. Integrated Analysis of Soil Metagenome and Soil Metabolome Reveals the Differential Responses of Sorghum and Peanut Rhizosphere Microbes to Salt Stress. *J. Soil Sci. Plant Nutr.* **2024**, *24*, 2959–2971. [CrossRef]
15. Yang, J.; Song, J.X.; Feng, Y.Y.; Cao, Y.M.; Fu, B.Z.; Zhang, Z.Q.; Ma, N.; Li, Q.; Hu, T.M.; Wang, Y.F.; et al. Osmotic stress-induced lignin synthesis is regulated at multiple levels in alfalfa (*Medicago sativa* L.). *Int. J. Biol. Macromol.* **2023**, *246*, 125501. [CrossRef] [PubMed]
16. Ghahramani Ghahramanloo, S.; Seyed Rahmani, R.; Karimbeigi, H.; Darvishzadeh, R. Meta-Analysis of Maize Adaptation to Salt Stress: Key Gene Expressions and Regulatory Pathways. *J. Plant Growth Regul.* **2025**, *44*, 5483–5495. [CrossRef]
17. Liu, J.C.; Li, S.Y.; Li, X.T.; Wang, H.Z.; Liu, P.; Zhang, J.W.; Zhao, B.; Ren, B.C.; Ren, H. Effects of salt stress on root growth and nutrient absorption efficiency of different salt-tolerant summer maize varieties. *Acta Agron. Sin.* **2026**, *52*, 565–577. [CrossRef]
18. Sun, S.Q.; Zhao, X.Q.; Li, X.; He, M.Y.; Wang, J.; Xiang, X.X.; Niu, Y. ZnONPs Alleviates Salt Stress in Maize Seedlings by Improving Antioxidant Defense and Photosynthesis Potential. *Plants* **2025**, *14*, 3104. [CrossRef] [PubMed]

19. Ju, T.; Yang, K.; Ji, D.; Chang, L.; Alquiza, M.d.J.P.; Li, Y. Microplastics influence nutrient content and quality of salt-affected agricultural soil under plastic mulch. *Environ. Res.* **2025**, *264*, 120376. [CrossRef] [PubMed]
20. Meng, C.R.; Yan, L.; Zhang, S.J.; Wei, C.Z. Variation of Soil Salinity in Plow Layer of Farm lands under Long-term Mulched Drip Irrigation in Arid Region. *Acta Pedol. Sin.* **2017**, *54*, 1386–1394. [CrossRef]
21. Xu, S.; Zhao, R.; Sun, J.; Sun, Y.H.; Xu, G.J.; Wang, F.Y. Microplastics change soil properties, plant performance, and bacterial communities in salt-affected soils. *J. Hazard. Mater.* **2024**, *471*, 134333. [CrossRef] [PubMed]
22. Liu, X.D.; Wang, Z.S.; Shi, G.Y.; Gao, Y.B.; Zhang, H.; Liu, K.C. Combined transcriptome and metabolome analysis revealed the toxicity mechanism of individual or combined of microplastic and salt stress on maize. *Ecotoxicol. Environ. Saf.* **2025**, *293*, 118034. [CrossRef] [PubMed]
23. Peng, Q.Y.; Shen, R.Q.; Li, X.Q.; Ye, T.; Dong, J.; Fu, Y.Y.; Yuan, W.P. A twenty-year dataset of high-resolution maize distribution in China. *Sci. Data* **2023**, *10*, 658. [CrossRef] [PubMed]
24. Velikova, V.; Yordanov, I.; Edreva, A. Oxidative stress and some antioxidant systems in acid rain-treated bean plants. *Plant Sci.* **2000**, *151*, 59–66. [CrossRef]
25. Liu, G.; Su, X.; Guan, L.; Hu, F. Comparison of Defensive Enzyme Activities in the Leaves of Seven Oriental Lily Hybrids after Inoculation with Botrytis elliptica. *J. Am. Soc. Hortic. Sci.* **2019**, *144*, 55–62. [CrossRef]
26. Karam, E.A.; Keramat, B.; Sorbo, S.; Maresca, V.; Asrar, Z.; Mozafari, H.; Basile, A. Interaction of triacontanol and arsenic on the ascorbate-glutathione cycle and their effects on the ultrastructure in *Coriandrum sativum* L. *Environ. Exp. Bot.* **2017**, *141*, 161–169. [CrossRef]
27. Hussain, F.; Hadi, F.; Rongliang, Q. Effects of Zinc Oxide Nanoparticles on Antioxidants, Chlorophyll Contents, and Proline in *Persicaria hydropiper* L. and Its Potential for Pb Phytoremediation. *Environ. Sci. Pollut. Res.* **2021**, *28*, 34697–34713. [CrossRef] [PubMed]
28. Li, B.; Dewey, C.N. RSEM: Accurate transcript quantification from RNA-Seq data with or without a reference genome. *BMC Bioinform.* **2011**, *12*, 323. [CrossRef] [PubMed]
29. Wang, L.; Feng, Z.; Wang, X.; Wang, X.; Zhang, X. DEGseq: An R package for identifying differentially expressed genes from RNA-seq data. *Bioinformatics* **2009**, *26*, 136–138. [CrossRef] [PubMed]
30. Bosker, T.; Bouwman, L.J.; Brun, N.R.; Behrens, P.; Vijver, M.G. Microplastics accumulate on pores in seed capsule and delay germination and root growth of the terrestrial vascular plant *Lepidium sativum*. *Chemosphere* **2019**, *226*, 774–781. [CrossRef] [PubMed]
31. de Souza Machado, A.A.; Lau, C.W.; Kloas, W.; Bergmann, J.; Bachelier, J.B.; Faltin, E.; Becker, R.; Görlich, A.S.; Rillig, M.C. Microplastics Can Change Soil Properties and Affect Plant Performance. *Environ. Sci. Technol.* **2019**, *53*, 6044–6052. [CrossRef] [PubMed]
32. Jiang, X.; Chen, H.; Liao, Y.; Ye, Z.; Li, M.; Klobučar, G. Ecotoxicity and genotoxicity of polystyrene microplastics on higher plant Vicia faba. *Environ. Pollut.* **2019**, *250*, 831–838. [CrossRef] [PubMed]
33. Guo, M.; Zhao, F.; Tian, L.; Ni, K.; Lu, Y.; Borah, P. Effects of polystyrene microplastics on the seed germination of herbaceous ornamental plants. *Sci. Total Environ.* **2021**, *809*, 151100. [CrossRef] [PubMed]
34. Shi, R.; Liu, W.; Lian, Y.; Wang, Q.; Zeb, A.; Tang, J. Phytotoxicity of polystyrene, polyethylene and polypropylene microplastics on tomato (*Lycopersicon esculentum* L.). *J. Environ. Manag.* **2022**, *317*, 115441. [CrossRef]
35. Yuan, W.K.; Zhou, Y.F.; Chen, Y.L.; Liu, X.N.; Wang, J. Toxicological effects of microplastics and heavy metals on the Daphnia magna. *Sci. Total Environ.* **2020**, *746*, 141254. [CrossRef] [PubMed]
36. Liu, Y.Q.; Chen, Y.; Li, Y.Y.; Ding, C.Y.; Li, B.L.; Han, H.; Chen, Z.J. Plant growth-promoting bacteria improve the Cd phytoremediation efficiency of soils contaminated with PE–Cd complex pollution by influencing the rhizosphere microbiome of sorghum. *J. Hazard. Mater.* **2024**, *469*, 134085. [CrossRef] [PubMed]
37. Yang, R.C.; Chen, M.J.; Cheng, L.; Cui, Y.L.; Li, C.Y.; Zhang, Y.Q. Molecular mechanisms underlying microplastics-induced inhibition of lateral root development in tomato (*Solanum lycopersicum* L.). *J. Environ. Manag.* **2025**, *395*, 127848. [CrossRef] [PubMed]
38. Giolai, M.; Laine, A.L. A trade-off between investment in molecular defense repertoires and growth in plants. *Science* **2024**, *386*, 677–680. [CrossRef] [PubMed]
39. Ni, G.Y.; Zhao, P.; Ye, Y.H.; Zhu, L.W.; Hou, Y.P.; Huang, Q.Q.; Wei, W.; Ouyang, L. High photosynthetic capacity and energy-use efficiency benefit both growth and chemical defense in invasive plants. *Chemoecology* **2020**, *30*, 69–78. [CrossRef]
40. Shi, B.H.; Li, K.; Xu, R.; Zhang, F.; Yu, Z.P.; Ding, Z.J.; Tian, H.Y. Methionine-mediated trade-off between plant growth and salt tolerance. *Plant Physiol.* **2025**, *197*, kiaf074. [CrossRef] [PubMed]
41. Liu, Y.Y.; Guo, R.; Zhang, S.W.; Sun, Y.H.; Wang, F.Y. Uptake and translocation of nano/microplastics by rice seedlings: Evidence from a hydroponic experiment. *J. Hazard. Mater.* **2021**, *421*, 126700. [CrossRef] [PubMed]

42. Zhang, S.L.; Zhang, F.C.; Cai, L.; Xu, N.; Zhang, C.; Yadav, V.; Zhou, X.M.; Wu, X.Y.; Zhong, H.X. Visual observation of polystyrene nano-plastics in grape seedlings of Thompson Seedless and assessing their effects via transcriptomics and metabolomics. *J. Hazard. Mater.* **2024**, *478*, 135550. [CrossRef] [PubMed]
43. Zhang, Y.; Yang, X.; Luo, Z.X.; Lai, J.L.; Li, C.; Luo, X.G. Effects of polystyrene nanoplastics (PSNPs) on the physiology and molecular metabolism of corn (*Zea mays* L.) seedlings. *Sci. Total Environ.* **2022**, *806*, 150895. [CrossRef] [PubMed]
44. Zhang, P.; Guo, Z.L.; Luo, W.H.; Monikh, F.A.; Xie, C.J.; Valsami-Jones, E.; Lynch, I.; Zhang, Z.Y. Graphene Oxide-Induced pH Alteration, Iron Overload, and Subsequent Oxidative Damage in Rice (*Oryza sativa* L.): A New Mechanism of Nanomaterial Phytotoxicity. *Environ. Sci. Technol.* **2020**, *54*, 3181–3190. [CrossRef] [PubMed]
45. Hasanuzzaman, M.; Raihan, M.d.R.H.; Masud, A.A.C.; Rahman, K.; Nowroz, F.; Rahman, M.; Nahar, K.; Fujita, M. Regulation of Reactive Oxygen Species and Antioxidant Defense in Plants under Salinity. *Int. J. Mol. Sci.* **2021**, *22*, 9326. [CrossRef] [PubMed]
46. Iqbal, N.; Khan, V.; Singh, R.; Saffeullah, P.; Umar, S.; Gupta, R. Reactive Oxygen Species and Glutathione-Mediated Regulation of Phytohormone Signaling in the Activation of Plant Immunity. *J. Plant Growth Regul.* **2025**, *45*, 1661–1676. [CrossRef]
47. Wang, C.R.; Tian, Y.; Wang, X.R.; Geng, J.J.; Jiang, J.L.; Yu, H.X.; Wang, C. Lead-contaminated soil induced oxidative stress, defense response and its indicative biomarkers in roots of Vicia faba seedlings. *Ecotoxicology* **2010**, *19*, 1130–1139. [CrossRef] [PubMed]
48. Martín, C.; Pirredda, M.; Fajardo, C.; Costa, G.; Sánchez-Fortún, S.; Nande, M.; Mengs, G.; Martín, M. Transcriptomic and physiological effects of polyethylene microplastics on Zea mays seedlings and their role as a vector for organic pollutants. *Chemosphere* **2023**, *322*, 138167. [CrossRef] [PubMed]
49. Wang, J.Y.; Lu, S.Y.; Guo, L.Q.; Wang, P.; He, C.G.; Liu, D.; Bian, H.F.; Sheng, L.X. Effects of polystyrene nanoplastics with different functional groups on rice (*Oryza sativa* L.) seedlings: Combined transcriptome, enzymology, and physiology. *Sci. Total Environ.* **2022**, *834*, 155092. [CrossRef] [PubMed]
50. He, Z.; Webster, S.; He, S.Y. Growth–defense trade-offs in plants. *Curr. Biol.* **2022**, *32*, R634–R639. [CrossRef] [PubMed]
51. Cannea, F.B.; Padiglia, A. Antioxidant Defense Systems in Plants: Mechanisms, Regulation, and Biotechnological Strategies for Enhanced Oxidative Stress Tolerance. *Life* **2025**, *15*, 1293. [CrossRef] [PubMed]

Disclaimer/Publisher's Note: The statements, opinions and data contained in all publications are solely those of the individual author(s) and contributor(s) and not of MDPI and/or the editor(s). MDPI and/or the editor(s) disclaim responsibility for any injury to people or property resulting from any ideas, methods, instructions or products referred to in the content.